Journal of The Electrochemical Society, **153** (7) A1302-A1309 (2006)
0013-4651/2006/153(7)/A1302/8/$20.00 © The Electrochemical Society

Stability of Materials as Candidates for Sulfur-Resistant Anodes of Solid Oxide Fuel Cells

Zhe Cheng,* Shaowu Zha, and Meilin Liu**,z**

School of Materials Science and Engineering, Georgia Institute of Technology, Atlanta, Georgia 30332, USA

Development of sulfur-resistant anode materials for solid oxide fuel cells (SOFCs) is critical to cost reduction of SOFC technologies. In this paper, we report the thermodynamic stability of various candidate materials for sulfur-resistant anodes of SOFCs, including metal carbides, borides, nitrides, silicides, perovskite-structured oxides, and transition metal sulfides. The most probable reaction between each candidate material and hydrogen sulfide (H_2S)-containing fuels under SOFC operating conditions (i.e., high temperature, reducing atmosphere with significant concentration of water vapor) were predicted and compared with experimental observations. It was found that proper thermodynamic analysis provided accurate prediction of the stability for a wide range of materials and significantly reduced the number of candidate materials for further in-depth study.
 [DOI: 10.1149/1.2198107]

Manuscript submitted December 22, 2005; revised manuscript received March 13, 2006. Available electronically May 5, 2006.

Effective utilization of sulfur-containing fuels in solid oxide fuel cells (SOFCs) has generated great interest in the development of sulfur-resistant anode materials for SOFCs. Previous studies on sulfur-tolerant anode materials can be grouped into two categories—those for SOFCs exposed to fuels with very high concentration (~5–100 vol %) of H_2S[1-10]) and those exposed to fuels with H_2S in parts per million range.[11-14] These studies are of great importance because they may lead to the elimination of the desulfurization system in the current SOFC fuel-processing unit, which would significantly simplify operation and reduce the cost. To date, unfortunately, the selection of sulfur-resistant anode materials seems to be largely in a trial-and-error manner: potential candidate material is fabricated as the anode in an SOFC and tested in sulfur-containing fuel. Though straightforward, it is often found that the candidate material simply transformed into other phases upon exposure to H_2S-containing fuels[3,4] and failed due to loss of structural integrity. One effective tool to guide the selection of sulfur-resistant anode materials is to analyze the thermodynamic stability of the candidate materials. Thermodynamics has been used to analyze the stability of cathode and interconnect materials for SOFCs.[15,16] For the study of sulfur-resistant anodes, this involves predicting whether the material will react with H_2S, water vapor, or other cell components and whether the material will melt or evaporate in SOFC anode environments. Such a method is expected to be of great importance, because in real SOFCs, the porous anodes are subject to high temperatures ($\geqslant$700°C) for years and the materials stability would most likely be determined by thermodynamics. Prediction of the materials stability based on thermodynamics could help researchers avoid a large number of trial experiments and identify the most promising candidate in a much more efficient way. However, thermodynamic stability is a necessary but not sufficient condition for a viable sulfur-tolerant anode material; it must have other desirable properties, including adequate electrical conductivity, high catalytic activity for fuel oxidation, as well as compatibility with other cell components such as electrolyte and interconnect. In addition, stability of surface species (e.g., adsorbates) is not included in the thermodynamic analysis for bulk materials. The adsorption of sulfur-containing species on anode surfaces is being studied using quantum-chemical calculations.[17]

In this paper, we report the results of our thermodynamic analysis on the stability of several classes of candidate sulfur-resistant anode materials. The most probable reactions that could cause failure of the candidates are identified. For the most typical materials of each class, the predictions are compared with experimental observations. The limitations of the thermodynamic analysis are also discussed at the end and the directions for future research are pointed out.

* Electrochemical Society Student Member.
** Electrochemical Society Active Member.
z E-mail: meilin.liu@mse.gatech.edu

Thermodynamic Analysis

The thermochemical data for simple compounds investigated in this study were taken from standard references.[18,19] The thermochemical data for most ABO_3 perovskites are not documented and were estimated from empirical equations in the literature. The estimation is valid because it is known that the enthalpy change for the reaction from simple oxides to complex oxides has close dependence on their structure.[20-26] For the example of ABO_3 perovskites, Navrotsky reported a good linear relationship between the reaction enthalpy for the formation of $A^{2+}B^{4+}O_3$ from AO and BO_2 simple oxides and the Goldschmidt tolerance factor (t_p) of the perovskite structure, which is defined as

$$t_p = \frac{r_A + r_O}{\sqrt{2}(r_B + r_O)} \quad [1]$$

where r_A, r_B, and r_O are the radii of A, B, and oxygen ions, respectively.[20] It was proposed that Shannon's effective radii for A-site ions in 12-coordination state and for B-site ions in 6-coordination state should be used to calculate t_p.[20,27] Later, Yokokawa et al.[21] did similar analysis and found that the reaction enthalpy for the formation of $A^{3+}B^{3+}O_3$ oxide from corresponding simple oxides

$$\tfrac{1}{2}A_2O_3 + \tfrac{1}{2}B_2O_3 = ABO_3 \quad [2]$$

could be approximated by

$$\Delta H_r^{\text{oxide}} = 630 - 720t_p \text{ kJ/mol} \quad [3]$$

while the reaction enthalpy for the formation of $A^{2+}B^{4+}O_3$ oxide from reaction

$$AO + BO_2 = ABO_3 \quad [4]$$

or

$$AO + \tfrac{1}{2}B_2O_4 = ABO_3 \quad [5]$$

could be approximated by

$$\Delta H_r^{\text{oxide}} = 875 - 1000t_p \text{ kJ/mol} \quad [6]$$

Yokokawa and co-workers used these empirical equations in a series studies to analyze stability and the reactivity of perovskites with other materials like yttria-stabilized zirconia (YSZ) and demonstrated the applicability of these equations.[15,16,22] Recently, similar empirical relations were also proposed by Cheng and Navrotsky,[23] who found the reaction enthalpy for Reaction 2 could be approximated by

Table I. Starting materials and preparation methods for samples synthesized in this study.

Sample	Starting materials	Preparation method and final heat-treatment condition
β-SiC	Phenolic resin (775D69, Georgia Pacific) tetraethoxysilane (TEOS, Alfa Aesar)	Solution-based processing 1475 (4 h, Ar)
$LaTiO_3$	La_2O_3 (Aldrich, 99.9%) Ti_2O_3 (Alfa Aesar, 99.8%)	Solid-state reaction 1450 (5 h, 4% H_2/96% Ar), carbon covered
$LaVO_3$	La_2O_3 (Aldrich, 99.9%) V_2O_5 (Aldrich, 99.6%)	Solid-state reaction 1450 (5 h, 4% H_2/96% Ar)
$SrTiO_3$	$SrCO_3$ (Aldrich, 99.9%) rutile-TiO_2 (Alfa Aesar, 99.9%)	Solid-state reaction 1300 (2 h, air)
$SrVO_3$	$SrCO_3$ (Aldrich, 99.9%) V_2O_5 (Aldrich, 99.6%)	Solid-state reaction 1450 (5 h + 5 h, 4% H_2/96% Ar)

$$\Delta H_r^{\text{oxide}} = 323.8 - 389.3t_p \text{ kJ/mol} \quad [7]$$

and the reaction enthalpy for Reaction 4 or 5 could be approximated by

$$\Delta H_r^{\text{oxide}} = 844.4 - 956.0t_p \text{ kJ/mol} \quad [8]$$

In this paper, both $\Delta H_r^{\text{oxide}}$ values from Eq. 3 and 7 were calculated for Reaction 2 ($A^{3+}B^{3+}O_3$ oxide) and both $\Delta H_r^{\text{oxide}}$ values from Eq. 6 and 8 were calculated for Reaction 4 or 5 ($A^{2+}B^{4+}O_3$ oxide). Unless stated otherwise, the values calculated using Eq. 7 and 8 are given directly while the values calculated using Eq. 3 and 6 are listed in the brackets. The entropy change for the formation of complex-structured oxide (e.g., ABO_3 perovskite) from simple oxides, $\Delta S_r^{\text{oxide}}$, are usually very small (~0–5 J/mol K).[21] As a result, the contribution of the entropy change to the total free energy change ($T\Delta S_r^{\text{oxide}}$) was on the order of a few kJ/mol, which is usually much less than one tenth of the enthalpy change $\Delta H_r^{\text{oxide}}$.[21] Therefore, as a first approximation, the entropy term was omitted in the calculation of the free energy change for reactions from simple oxides to complex oxides (e.g., ABO_3, $A_2B_2O_7$), and $\Delta G_r^{\text{oxide}} = \Delta H_r^{\text{oxide}} - T\Delta S_r^{\text{oxide}} \approx \Delta H_r^{\text{oxide}}$.[16]

Experimental

Some of the samples used in this study were obtained from commercial suppliers: ZrC (99.5%) and WC (99.6%) were from Alfa Aesar, TiN (99%) was from Aldrich, and WS_2 (99.8%) was from Cerac, Inc. The rest were synthesized in the authors' lab. Table I lists the precursors and preparation methods used for the syntheses. Of the precursors, La_2O_3 and $SrCO_3$ were first calcinated in air at 800 and 300°C, respectively, for 2 h to remove the adsorbed moisture. All complex oxides were synthesized using a solid-state reaction method. The raw materials were mixed, ground for 1 h, pressed into pellets at 70 MPa, and heat-treated at high temperature. For some complex oxides like $SrVO_3$, grinding and calcination were repeated until complete reaction and uniform composition were achieved, as confirmed by X-ray diffraction (XRD, PW1800 X-ray diffractometor, Philips Analytical). The radiation source was Cu Kα lines. The

Table II. Melting point (T_m), electrical conductivity at 25°C (σ_{25}) and 800°C (σ_{800}), and CTE (25–1000°C) for some materials investigated in this study.

Material	T_m (°C)	σ_{25} (S cm^{-1})	σ_{800} (S cm^{-1})	CTE (10^{-6}/K)
B_4C[a]	2470	1.0×10^3	1.0×10^3	4.8–5.5
Cr_3C_2[a]	1800[b]	1.3×10^4	4.8×10^3	11.7
Mo_2C[a]	2500	1.4×10^4	3.6×10^3	7.3
β-SiC[a]	2986[b]	1.0	NA	3.8–5.8
TaC[a]	4000	4.6×10^4	2.5×10^4	7.1
TiC[a]	3017	5.0×10^3	2.1×10^3	8.0
WC[a]	2800[b]	5.2×10^4	3.8×10^4	5.8
W_2C[a]	2785	1.3×10^4	5.3×10^3	6.4–8.1
ZrC[a]	3532	1.3×10^4	5.9×10^3	7.0
TiB_2[a]	2920	1.1×10^5	4.4×10^4	4.6
ZrB_2[a]	3050	1.0×10^5	3.7×10^4	5.9
CrN[a]	1500[b]	1.6×10^3	NA	0.7–3.1
TiN[a]	2950	2.5×10^4	1.9×10^4	8.1–9.0
VN[a]	2177	1.7×10^4	1.6×10^4	8.1
ZrN[a]	2952	5.6×10^4	2.2×10^4	7.0
$MoSi_2$[a]	2280	4.6×10^4	7.8×10^3	8.2
$La_{0.4}Sr_{0.6}TiO_3$[c]	>1600	6.0×10^3	5.0×10^2	11–12
$La_{0.7}Sr_{0.3}VO_3$[d]	>1600	7.0×10^2	1.5×10^2	9.6–11.5
$La_{0.75}Sr_{0.25}Cr_{0.5}Mn_{0.5}O_3$[e,f]	>1600	NA	1.0	8.9–10.1
$Gd_2Ti_{1.4}Mo_{0.6}O_7$[g]	>1500	NA	5.0	NA

[a] From Ref. 29.
[b] Decomposition temperature.
[c] From Ref. 30.
[d] From Ref. 31.
[e] From Ref. 32.
[f] From Ref. 9.
[g] From Ref. 33.

Table III. Gibbs free energy change (ΔG_r) for the reaction between water vapor and transition metal carbides at 950°C. The partial pressure of H_2 and H_2O are fixed at 0.87 and 0.03, respectively, and the partial pressure of CO is 10^{-6} or 10^{-1}.

Reaction (written based on 1 mol H_2O)	$\Delta G_r(p_{CO} = 10^{-6})$ in kJ/mol	$\Delta G_r(p_{CO} = 10^{-1})$ in kJ/mol
$1/7\ B_4C_{(s)} + H_2O_{(g)} = 2/7\ B_2O_{3(1)} + 1/7\ CO_{(g)} + H_{2(g)}$	−106	−89
$2/13\ Cr_3C_{2(g)} + H_2O_{(g)} = 3/13\ Cr_2O_{3(s)} + 4/13\ CO_{(g)} + H_{2(g)}$	−69	−33
$MoC_{(s)} + H_2O_{(g)} = Mo_{(s)} + CO_{(g)} + H_{2(g)}$	−116	1
$Mo_2C_{(s)} + H_2O_{(g)} = 2\ Mo_{(s)} + CO_{(g)} + H_{2(g)}$	−86	31
$1/3\ SiC_{(s,beta)} + H_2O_{(g)} = 1/3\ SiO_{2(s,cristobalite)} + 1/3\ CO_{(g)} + H_{2(g)}$	−115	−76
$2/7\ TaC_{(s)} + H_2O_{(g)} = 1/7\ Ta_2O_{5(s)} + 2/7\ CO_{(g)} + H_{2(g)}$	−64	−31
$1/3\ TiC_{(s)} + H_2O_{(g)} = 1/3\ TiO_{2(s,rutile)} + 1/3\ CO_{(g)} + H_{2(g)}$	−90	−51
$WC_{(s)} + H_2O_{(g)} = W_{(s)} + CO_{(g)} + H_{2(g)}$	−111	6
$W_2C_{(s)} + H_2O_{(g)} = 2\ W_{(s)} + CO_{(g)} + H_{2(g)}$	−120	−2
$1/3\ ZrC_{(s)} + H_2O_{(g)} = 1/3\ ZrO_{2(s)} + 1/3\ CO_{(g)} + H_{2(g)}$	−133	−94

SiC powder was synthesized using a solution-based process.[28] To verify the prediction of the materials' stability by thermodynamics, representative materials were exposed to fuels containing H_2S at high temperature (usually 950°C) for 2–5 days. The nominal composition (by volume) of the fuels was either 10% H_2S/3% H_2O/87% H_2 or 50 ppm H_2S/50% H_2/1.5% H_2O/48.5% N_2.

Results

Metal carbides.— Many transition metal carbides have a very high melting point and excellent electrical conductivity.[29] Listed in Table II are the melting point, electrical conductivity, and CTE for some of the most common metal carbides. Some of the metal carbide materials such as Mo_2C have been reported to have good catalytic activity for various chemical reactions and, unlike metal catalyst, have the potential advantage of preventing carbon deposition (see Ref. 34 for a summary of using metal carbide as catalysts). However, the suitability of these materials as candidate sulfur-resistant anode materials for SOFCs is yet to be determined. Because SOFC anode is likely exposed to fuels containing various amounts of water vapor, one possible reaction that may lead to the failure of metal carbide anode is

$$M_xC_y + (y + z)H_2O = M_xO_z + yCO + (y + z)H_2 \quad [9]$$

If the elemental metal is more stable than the corresponding metal oxides in reducing atmosphere (such as molybdenum and tungsten), the reaction may be written as

$$M_xC_y + yH_2O = xM + yCO + yH_2 \quad [10]$$

Table III lists the free energy change for the hydrolysis of some common metal carbide materials at 950°C in fuels with different CO concentrations. For most carbides except molybdenum and tungsten carbide, the hydrolysis reaction is an energetically favorable process over a wide CO partial pressure range (e.g., 10^{-6}–10^{-1}). The hydrolysis reactions become even more energetically favorable as the CO concentration decreases or the water vapor concentration increases.

If the H_2S concentration is high (e.g., on the percentage range), the carbides may also react with H_2S to form metal sulfides as follows

$$M_xC_y + zH_2S + yH_2O = M_xS_z + yCO + (z + y)H_2 \quad [11]$$

This reaction is a complex one involving three reactants and three products. Even if it happens, the real scenario might be that the carbides are first hydrolyzed as in Reaction 9 or 10, then the hydrolysis product (metal oxides or metal) reacts with H_2S to form metal sulfides, e.g.

$$M_xO_z + yH_2S + (z - y)H_2 = M_xS_y + zH_2O \quad [12]$$

or

$$xM + yH_2S = M_xS_y + yH_2 \quad [13]$$

In terms of thermodynamics, to predict whether hydrolysis (Reaction 9 or 10) or sulfidation (Reaction 11) will happen, it is sufficient to evaluate the free energy change for Reaction 12 or 13. If the free energy change is negative, it is possible that metal sulfide will be the final product; if the free energy change is positive, the metal oxide or metal from hydrolysis will be the final product. Table IV lists the free energy change for the sulfidation of some hydrolysis product from carbides in fuels with different concentration of H_2S. Except for Mo and W in fuels with high concentration of H_2S, the free energy change for all the reactions is positive, indicating the metal oxide or metal from the hydrolysis will be the final product. Therefore, from the above thermodynamic analysis, most metal carbide materials are ruled out as sulfur-resistant anodes of SOFCs because of their poor resistance to water vapor in the fuel gas.

To verify the prediction by thermodynamics, several materials including β-SiC, ZrC, and WC were exposed to a gas mixture of 10% H_2S/3% H_2O/87% H_2 at 950°C for 2–5 days. The CO concentration in the fuel was ~1 ppm. Figure 1-3 show the comparison of the X-ray diffraction (XRD) patterns for β-SiC, ZrC, and WC before and after the stability test. As predicted, the hydrolysis of β-SiC and ZrC were observed: β-SiC transformed to silica (cristo-

Table IV. Free energy change for the reaction between H_2S and hydrolysis product of metal carbides (i.e., oxides and metals) at 950°C. The partial pressure of H_2 and H_2O were fixed at 0.87 and 0.03, respectively.

Reaction (written based on 1 mol H_2S)	$\Delta G_r\ (p_{H_2S} = 5 \times 10^{-5})$ in kJ/mol	$\Delta G_r\ (p_{H_2S} = 10^{-1})$ in kJ/mol
$0.5\ Cr_2O_{3(s)} + H_2S_{(g)} + 0.5\ H_{2(g)} = CrS_{(s)} + 1.5\ H_2O_{(g)}$	77	−0.1
$0.5\ Mo_{(s)} + H_2S_{(g)} = 0.5\ MoS_{2(s)} + H_{2(g)}$	41	−36
$0.5\ SiO_{2(s,cristobalite)} + H_2S_{(g)} = 0.5\ SiS_{2(s)} + H_2O_{(g)}$	183	105
$0.5\ TiO_{2(s,rutile)} + H_2S_{(g)} = 0.5\ TiS_{2(s,rutile)} + H_2O_{(g)}$	102[a]	39[a]
$0.5\ W_{(s)} + H_2S_{(g)} = 0.5\ WS_{2(s)} + H_{2(g)}$	50	−27
$0.5\ ZrO_{2(s,monoclinic)} + H_2S_{(g)} = 0.5\ ZrS_{2(s)} + H_2O_{(g)}$	107	30

[a] Values at 727°C.

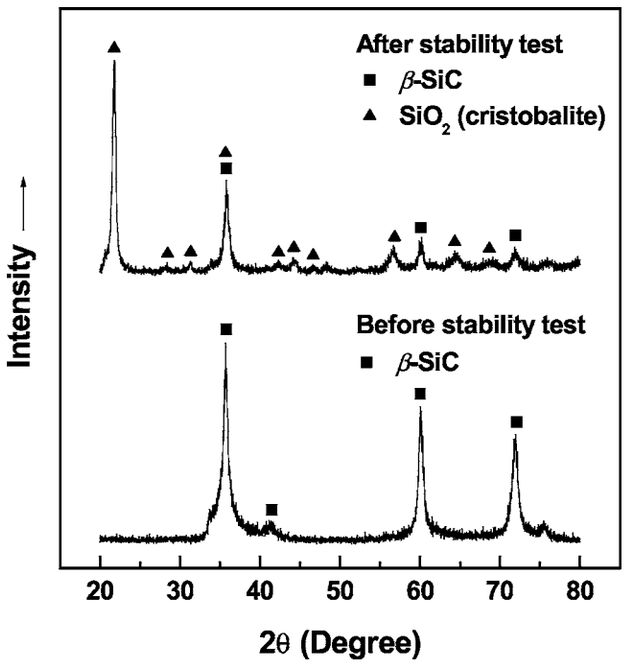

Figure 1. XRD patterns for the β-SiC sample before and after exposure to 10% H_2S/3% H_2O/87% H_2 at 950°C for 5 days.

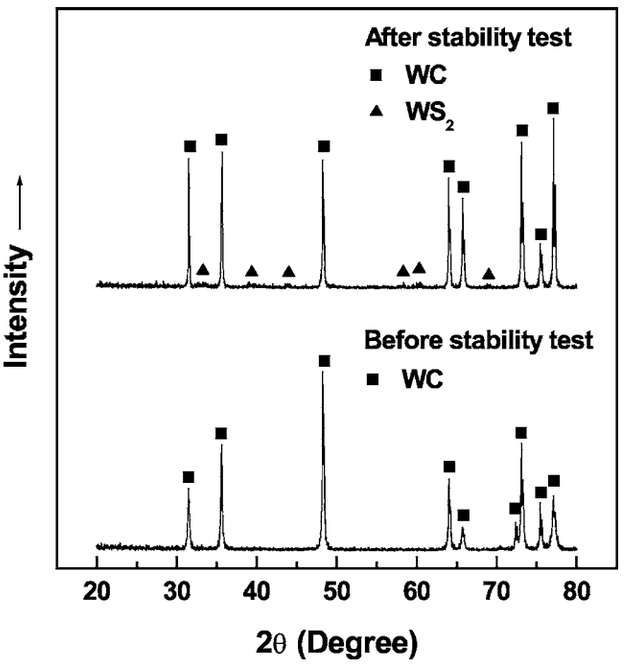

Figure 3. XRD patterns for the WC sample before and after exposure to 10% H_2S/3%/87% H_2 at 950°C for 2 days.

balite phase) and ZrC transformed to monoclinic zirconia. For WC, although most of the materials did not change, XRD identified trace amount of WS_2, which was confirmed by the appearance of strong Raman bands corresponding to WS_2, as shown in Fig. 4 for the postexposure sample.

Metal borides, nitrides, and silicides.— Similar to the transition metal carbides, many transition metal borides, nitrides, and silicides also have high melting points, good electrical conductivity (see Table II), and better oxidation resistance than metal carbides.[29] However, thermodynamic analysis shows that hydrolysis is still a serious problem for these materials. Table V shows the free energy change for the hydrolysis of several common metal borides, nitrides, and silicides. All these reactions are energetically favorable. Like transition metal carbides, the reaction of these materials with H_2S could still be regarded as two steps with the first one as hydrolysis and the second as sulfidation of the corresponding hydrolysis prod-

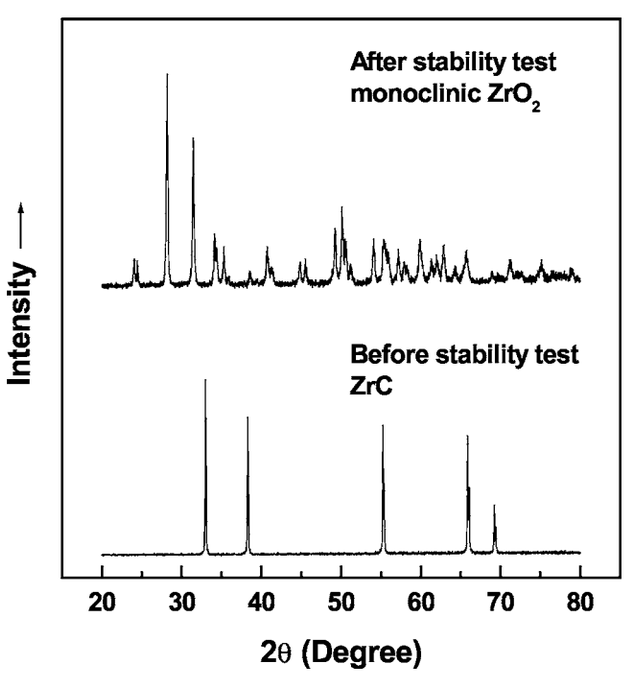

Figure 2. XRD patterns for the ZrC sample before and after exposure to 10% H_2S/3% H_2O/87% H_2 at 950°C for 5 days.

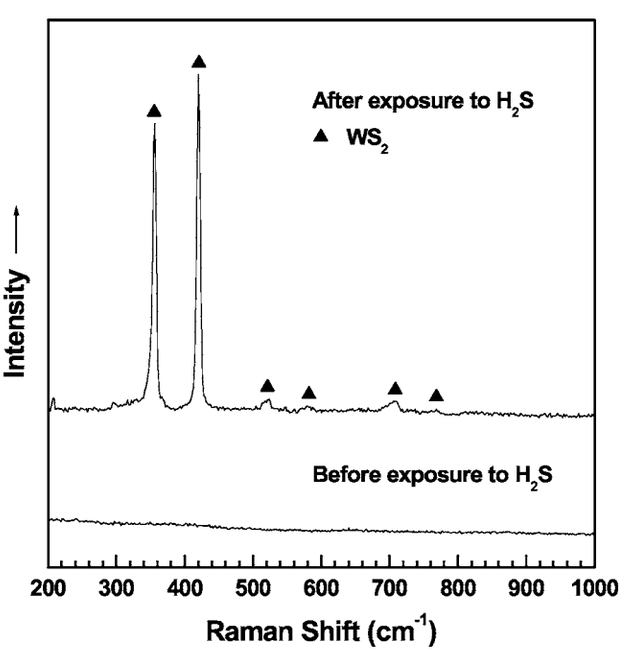

Figure 4. Raman spectra of the WC sample before and after exposure to 10% H_2S/3% H_2O/87% H_2 at 950°C for 2 days.

Table V. Free energy change for the reaction between water vapor and transition metal borides (M_xB_y), nitrides (M_xN_y), and silicide (M_xSi_y) at 950°C. The partial pressure of H_2 and H_2O are fixed at 0.87 and 0.03, respectively.

Reaction (written based on 1 mol H_2O)	ΔG_r (kJ/mol)
$0.2\ TiB_{2(s)} + H_2O_{(g)} = 0.2\ TiO_{2(s)} + 0.2\ B_2O_{3(1)} + H_{2(g)}$	−72
$0.2\ ZrB_{2(s)} + H_2O_{(g)} = 0.2\ ZrO_{2(s)} + 0.2\ B_2O_{3(1)} + H_{2(g)}$	−93
$2/3\ CrN_{(s)} + H_2O_{(g)} = 1/3\ Cr_2O_{3(s)} + 1/3\ N_{2(g)} + H_{2(g)}$	−88[a]
$0.5\ TiN_{(s)} + H_2O_{(g)} = 0.5\ TiO_{2(s,rutile)} + 0.25\ N_{2(g)} + H_{2(g)}$	−71[a]
$2/3\ VN_{(s)} + H_2O_{(g)} = 1/3\ V_2O_{3(s)} + 1/3\ N_{2(g)} + H_{2(g)}$	−60[a]
$0.5\ ZrN_{(s)} + H_2O_{(g)} = 0.5\ ZrO_{2(s)} + 0.25\ N_{2(g)} + H_{2(g)}$	−129[a]
$0.25\ MoSi_{2(s)} + H_2O_{(g)} = 0.25\ Mo_{(s)} + 0.5\ SiO_{2(s)} + H_{2(g)}$	−102

[a] Partial pressure of N_2 is 10^{-6}.

ucts. Nevertheless, unless inhibited by extremely slow kinetics, the hydrolysis reactions will happen and none of those materials is going to survive in typical SOFC anode atmosphere. As an experimental verification, Fig. 5 shows the comparison of the XRD patterns of TiN powder before and after exposure to 10% H_2S/3% H_2O/87% H_2 fuel mixture at 950°C for 2 days. As predicted from thermodynamics, TiO_2 (rutile phase) was the only solid product after the exposure. Therefore, these borides, nitrides, and silicides are also ruled out as sulfur-resistant anode for SOFCs.

Complex oxides.— Metal oxides, especially those with complex structure, have been studied as candidate materials for sulfur-resistant anodes of SOFCs.[7-14,31] Some of them have a combination of desirable properties for anodes including reasonable electrical conductivity and close match of coefficients of thermal expansion (CTE) with other cell components (see Table II). To date, however, the determination of chemical stability (especially sulfur resistance) for these materials depends largely on experiments, i.e., the materials are exposed to H_2S-containing fuels at high temperature and the phase change is analyzed afterward.[4,9,31] A more efficient way is to predict their stability from the free energy change for the reaction of interest (e.g., sulfidation). In the following, examples of analyzing

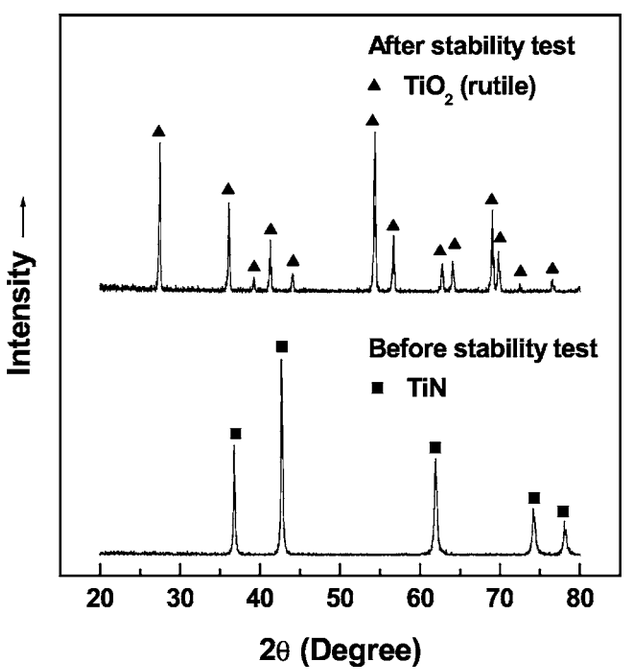

Figure 5. XRD patterns for the TiN sample before and after exposure to 10% H_2S/3% H_2O/87% H_2 at 950°C for 2 days.

the chemical stability for several perovskite-structured oxides are given, the majority of which show excellent agreement with experiments.

The $La_{1-x}Sr_xTiO_3$ materials have been reported as candidate sulfur-resistant anode materials in fuels with H_2S in the ~25–1000 ppm range.[13,14] However, the chemical resistance of this material to H_2S has not been reported. In this study, the chemical stability of $LaTiO_3$ and $SrTiO_3$, the two end compositions of the $La_{1-x}Sr_xTiO_3$ family, was analyzed. For $LaTiO_3$, because Ti has +3 valence, the oxidation of $LaTiO_3$ via

$$2LaTiO_{3(s)} + H_2O_{(g)} = La_2Ti_2O_{7(s)} + H_{2(g)} \quad [14]$$

is possible. The tolerance factor t_p for $LaTiO_3$ calculated from Eq. 1 is 0.943. Therefore, for the formation of $LaTiO_3$ from simple oxides

$$\tfrac{1}{2}La_2O_{3(s)} + \tfrac{1}{2}Ti_2O_{3(s)} \rightarrow LaTiO_{3(s)} \quad [15]$$

the enthalpy change, $\Delta H_r^{\text{oxide}}$ ($LaTiO_3$), calculated from Eq. 7, is −43.3 kJ/mol (−49.0 kJ/mol if Eq. 3 is used). As stated before, the entropy change for reactions like Eq. 15 is usually very small and the entropy contribution to the free energy change ($T\Delta S_r^{\text{oxide}}$) was neglected. Therefore, the Gibbs formation energy of $LaTiO_3$ could be estimated

$$\Delta G_f^{\text{O}}(LaTiO_3) \approx 0.5\Delta G_f^{\text{O}}(La_2O_3) + 0.5\Delta G_f^{\text{O}}(Ti_2O_3) + \Delta H_r^{\text{oxide}}(LaTiO_3) \quad [16]$$

Assuming that the reaction enthalpy for Reaction 15 is independent of temperature, at 950°C, $\Delta G_f^{\text{O}}(LaTiO_3) = -1358.2$ kJ/mol (−1363.9 kJ/mol if $\Delta H_r^{\text{oxide}}$ from Eq. 3 is used). For $La_2Ti_2O_7$, the enthalpy change for reaction

$$La_2O_{3(s)} + 2TiO_{2(s)} = La_2Ti_2O_{7(s)} \quad [17]$$

was −206.0 kJ/mol.[24] The standard Gibbs formation energy of $La_2Ti_2O_7$ would be

$$\Delta G_f^{\text{O}}(La_2Ti_2O_7) \approx \Delta G_f^{\text{O}}(La_2O_3) + 2\Delta G_f^{\text{O}}(TiO_2) + \Delta H_r^{\text{oxide}}(La_2Ti_2O_7) \quad [18]$$

At 950°C, $\Delta G_f^{\text{O}}(La_2Ti_2O_7) = -3098.0$ kJ/mol. Therefore, the change in Gibbs free energy for Reaction 14 is given by

$$\Delta G_r = \Delta G_f^{\text{O}}(La_2Ti_2O_7) + \Delta G_f^{\text{O}}(H_2) - 2\Delta G_f^{\text{O}}(LaTiO_3) - \Delta G_f^{\text{O}}(H_2O) + RT\ln\frac{p_{H_2}}{p_{H_2O}} \quad [19]$$

At 950°C in fuel of 10% H_2S/3% H_2O/87% H_2, $\Delta G_r = -167.2$ kJ/mol (−155.8 kJ/mol if $\Delta H_r^{\text{oxide}}$ from Eq. 3 is used). Therefore, Reaction 14 is a highly energetically favorable process. The free energy change for the reaction between $LaTiO_3$ and H_2S

$$2/3LaTiO_{3(s)} + H_2S_{(g)} = 1/3La_2S_{3(s)} + 2/3TiO_{2(s)} + 1/3H_{2(g)} + 2/3H_2O_{(g)} \quad [20]$$

under the same condition was calculated to be $\Delta G_r = -23.9$ kJ/mol (−20.1 kJ/mol if $\Delta H_r^{\text{oxide}}$ from Eq. 3 is used), indicating it is also a spontaneous process. However, the hydrolysis (Reaction 14) is more likely to happen because it is more energetically favorable and only involves oxidation instead of both sulfidation and phase separation as in the sulfidation Reaction 20.

For $SrTiO_3$, the standard Gibbs formation energy is available in the literature.[19] Because both Sr^{2+} and Ti^{4+} are stable against oxidation/reduction, the only possible reaction is sulfidation. Because no transformation of TiO_2 to titanium sulfide was observed in experiment (see Fig. 5) at 950°C in fuels with 10% H_2S, the sulfidation reaction of $SrTiO_3$ should be

$$SrTiO_{3(s)} + H_2S_{(g)} = SrS_{(s)} + TiO_{2(s)} + H_2O_{(g)} \quad [21]$$

The free energy change for this reaction is given by

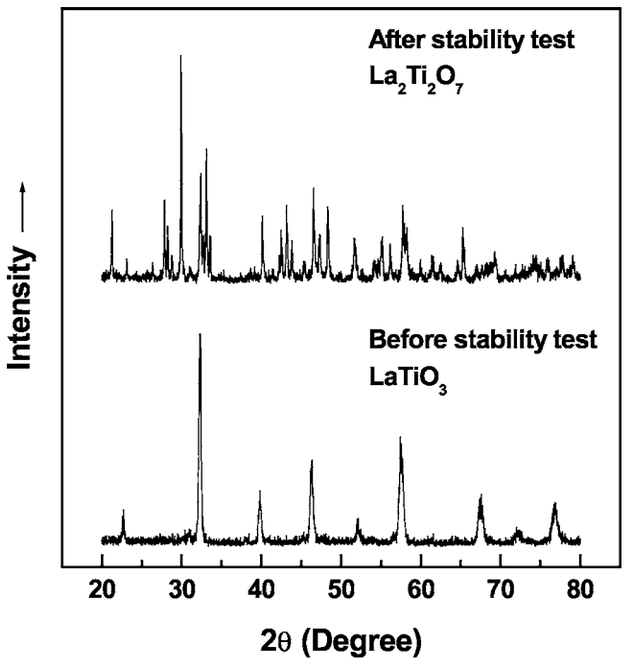

Figure 6. XRD patterns for the $LaTiO_3$ sample before and after exposure to 10% H_2S/3% H_2O/87% H_2 at 950°C for 5 days.

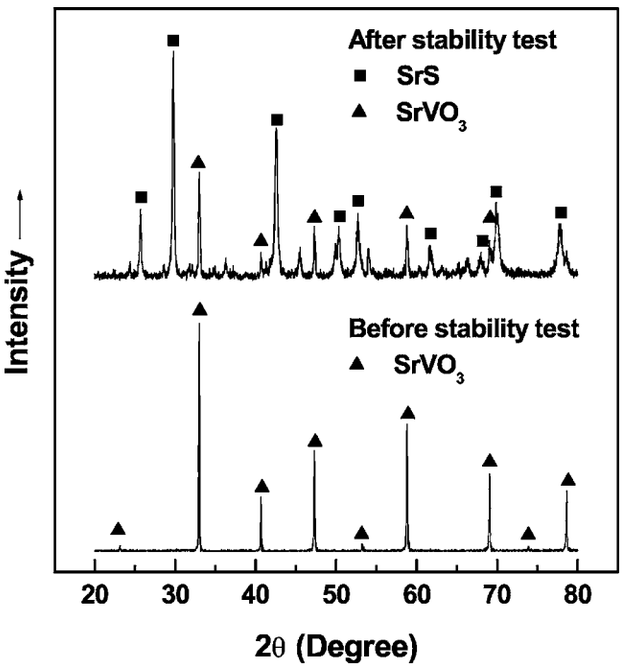

Figure 8. XRD patterns for the $SrVO_3$ sample before and after exposure to 10% H_2S/3% H_2O/87% H_2 at 950°C for 5 days.

$$\Delta G_r = \Delta G_f^{O}(SrS) + \Delta G_f^{O}(TiO_2) + \Delta G_f^{O}(H_2O) - \Delta G_f^{O}(SrTiO_3) - \Delta G_f^{O}(H_2S) + RT \ln \frac{p_{H_2O}}{p_{H_2S}} \quad [22]$$

At 950°C in fuel of 10% H_2S/3% H_2O/87% H_2, ΔG_r = 33.0 kJ/mol. Therefore, the sulfidation reaction will not happen. As a verification of the analysis made above, Fig. 6 and 7 show the XRD patterns of $LaTiO_3$ and $SrTiO_3$ before and after exposure to 10% H_2S/3% H_2O/87% H_2 at 950°C for 5 days. $LaTiO_3$ (JCPDS card no. 34-0596) was oxidized to $La_2Ti_2O_7$ (JCPDS card no. 28-0517) while no phase change was observed for $SrTiO_3$ (JCPDS card no. 35-0734).

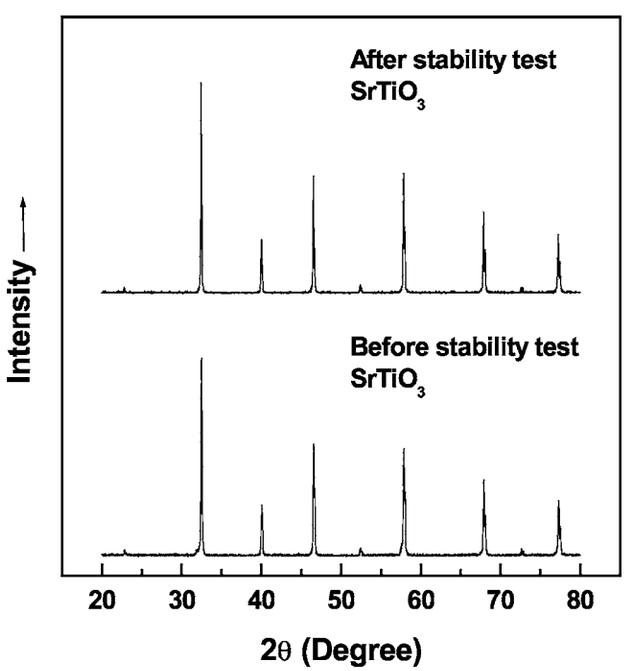

Figure 7. XRD patterns for the $SrTiO_3$ sample before and after exposure to 10% H_2S/3% H_2O/87% H_2 at 950°C for 5 days.

$La_{1-x}Sr_xVO_3$ is proposed as a candidate sulfur-resistant anode material for SOFCs that utilize fuels with H_2S concentration in the 5–10% range.[7,8,31] The two end compositions, $LaVO_3$ and $SrVO_3$, were also analyzed in this study. The tolerance factor, t_p, for $LaVO_3$ and $SrVO_3$ was 0.957 and 1.014, respectively. Similar to $LaTiO_3$, the estimated standard Gibbs formation energy at 950°C was −1226.1 kJ/mol for $LaVO_3$ and −1106.3 kJ/mol for $SrVO_3$ (−1236.3 kJ/mol and −1120.3 kJ/mol if ΔH_r^{oxide} values from Eq. 3 and 6 are used). For $SrVO_3$, the free energy change for the sulfidation reaction

$$SrVO_{3(s)} + H_2S_{(g)} + H_{2(g)} = SrS_{(s)} + 0.5V_2O_{3(s)} + 1.5H_2O_{(g)} \quad [23]$$

at 950°C in 10% H_2S/3% H_2O/87% H_2 is −29.2 kJ/mol (−15.2 kJ/mol if ΔH_r^{oxide} from Eq. 6 is used). Therefore, the sulfidation of $SrVO_3$ in fuels containing 10% H_2S can happen. Figure 8 compares the XRD patterns for the $SrVO_3$ sample before and after exposure to 10% H_2S/3% H_2O/87% H_2 at 950°C for 5 days. As predicted, the majority of $SrVO_3$ (JCPDS card no. 44-0039) transformed to SrS (JCPDS card no. 08-0489). For $LaVO_3$, the situation is slightly more complicated. The free energy change for the sulfidation reaction

$$2/3LaVO_{3(s)} + H_2S_{(g)} = 1/3La_2S_{3(s)} + 1/3V_2O_{3(s)} + H_2O_{(g)} \quad [24]$$

under similar conditions is very close to zero (−4.3 kJ/mol if ΔH_r^{oxide} from Eq. 7 is used and 2.5 kJ/mol if ΔH_r^{oxide} from Eq. 3 is used). Considering the uncertainty in the thermochemical data, it is concluded that this material is on the border of reaction because a small variation in experimental conditions (e.g., temperature or H_2S concentration) could lead to different results. In the exposure experiment, as shown in Fig. 9, we observed that after exposure to 10%

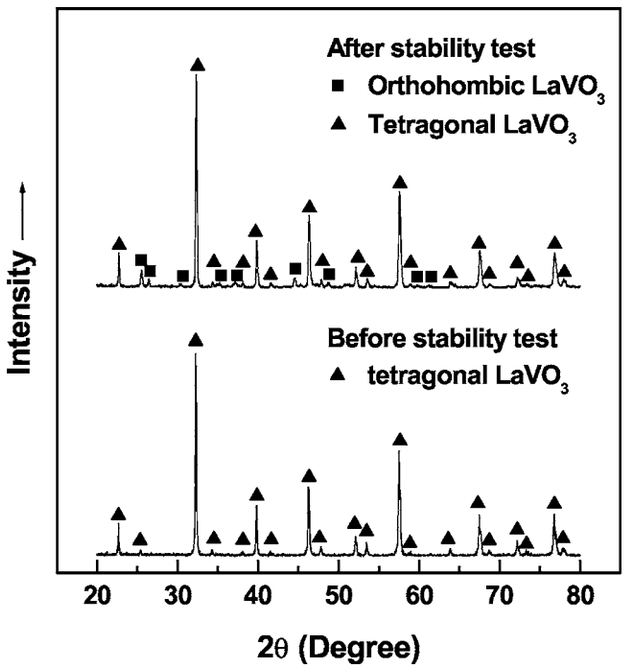

Figure 9. XRD patterns for the $LaVO_3$ sample before and after exposure to 10% H_2S/3% H_2O/87% H_2 at 950°C for 5 days.

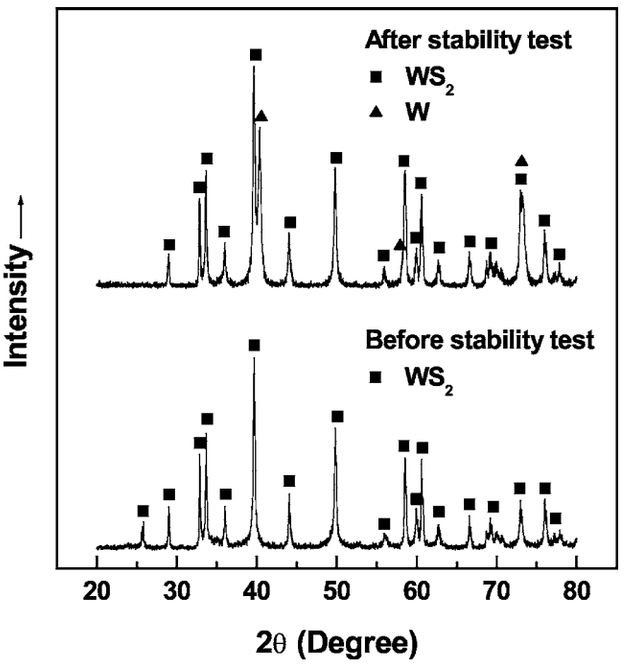

Figure 10. XRD patterns for the WS_2 sample before and after exposure to 50 ppm H_2S/50% H_2/1.5% H_2O/48.5% H_2 at 727°C for 12 h.

H_2S/3% H_2O/87% H_2 at 950°C for 5 days, $LaVO_3$ transformed partially from tetragonal structure (JCPDS card no. 11-0024) to orthorhombic structure (JCPDS card no. 36-0141).

Transition metal sulfides.— Transition metal sulfides seem a natural choice for sulfur-resistant anode materials; Mo and W-based sulfides have already been used for SOFCs that run on fuels with almost pure H_2S.[1-3,5,6] However, most bulk transition metal sulfides are not suitable candidates for sulfur-resistant anodes that only deal with H_2S in the parts per million range. For the example of WS_2, the calculated equilibrium pH_2S/pH_2 ratio at 727°C is 9.4×10^{-4}; bulk WS_2 is not going to be stable if pH_2S/pH_2 is only 1×10^{-4} in the fuel flow. In fact, as shown in Fig. 10, WS_2 powder decomposed partially into metal tungsten after exposure to a fuel of 50 ppm H_2S/50% H_2/1.5% H_2O/48.5% N_2 at 727°C for only 12 h.

Discussion

The reason metal carbides, borides, nitrides, and silicides are not resistant against hydrolysis is that the corresponding oxides (e.g., B_2O_3, SiO_2, TiO_2, Ta_2O_5, ZrO_2) are much more stable than the carbides, borides, nitrides, and silicides, even in SOFC anode atmosphere ($pO_2 \approx 10^{-18}$–10^{-20}). The only exceptions are W- and Mo-based carbide materials: the corresponding metal phase is more stable in reducing atmosphere and the free energy change for hydrolysis is rather small as long as the CO concentration is high and the water concentration is low. However, it is noted that the low CTE and high processing temperatures of these materials (i.e., Mo- and W-based carbides) may pose other challenges.

The reason for the difference in stability of perovskite oxides can be explained by comparison of the free energy change from simple oxides to complex oxides (i.e., $\Delta G_r^{\text{oxide}}$ for Reactions 2, 4, and 5, also called the stabilizing factor here) and the free energy change for the simple oxides to transform to other phases like sulfides (also called the disruptive factor here). For example, the stabilizing factor, $\Delta G_r^{\text{oxide}}$, for $SrTiO_3$ is −137.7 kJ/mol while the disruptive factor (ΔG_r for the sulfidation of SrO to SrS) under condition of the stability test (950°C, 10% H_2S/3% H_2O/87% H_2) is only −104.7 kJ/mol; therefore, $SrTiO_3$ will be stable. In comparison, for $LaTiO_3$, the stabilizing factor $\Delta G_r^{\text{oxide}} = -43.3$ kJ/mol (−49.0 kJ/mol if $\Delta H_r^{\text{oxide}}$ from Eq. 3 is used) while the disruptive factor includes two contributions—the oxidation of B-site simple oxide 1/2 Ti_2O_3 to TiO_2 ($\Delta G_r = -24.0$ kJ/mol at 950°C in 10% H_2S/87% H_2/3% H_2O) and the combination of TiO_2 with 1/2 La_2O_3 to form 1/2 $La_2Ti_2O_7$ ($\Delta G_r = -206/2 = -103.0$ kJ/mol).[24] The total disruptive factor has a ΔG_r of (−24.0) + (−103) = −127 kJ/mol, which is greater than the stability factor. Therefore, $LaTiO_3$ transformed to 1/2 $La_2Ti_2O_7$. Similarly, for $SrVO_3$, the stabilizing factor $\Delta G_r^{\text{oxide}} = -125.0$ kJ/mol (−139.0 kJ/mol if $\Delta H_r^{\text{oxide}}$ from Eq. 6 is used) while the disruptive factor also includes two contributions—the sulfidation of SrO to SrS (ΔG_r = −104.7 kJ/mol at 950°C in 10% H_2S/3% H_2O/87% H_2) and the reduction of 1/2 V_2O_4 to 1/2 V_2O_3 ($\Delta G_r = -49.5$ kJ/mol at 950°C in 10% H_2S/3% H_2O/87% H_2). The combined disruptive factor (−154.2 kJ/mol) is greater than the stabilizing factor, leading to the phase change under the test condition. The above discussion is also true for some other materials like doped $YFeO_3$, which had been tried as a sulfur-resistant anode.[4] Both of the simple oxides of A-site ion (Y_2O_3) and B-site ion (1/2 Fe_2O_3) could be sulfidized, and ΔG_r for the sulfidation of 1/2 Fe_2O_3 alone was −101 kJ/mol at 950°C in 10% H_2S/3% H_2O/87% H_2; the disruptive force is so large that the material will fail anyway in fuels with a high concentration of H_2S, as observed in the experiment.[4]

Despite the success with predicting the chemical stability of simple compounds and undoped perovskite-structured oxides, there is some uncertainty in the prediction of chemical stability for doped perovskites. For example, experiments showed that $La_{0.35}Sr_{0.65}TiO_3$ and $La_{1-x}Sr_xVO_3$ (x = 0.3, 0.5, and 0.7) were stable against both hydrolysis and sulfidation at 950°C in 10% H_2S/3% H_2O/87% H_2.[31] However, how to estimate the thermochemical data for these materials is unclear. Yokokawa et al. suggested that that the reaction enthalpy for materials like $LaMg_{0.5}Cr_{0.5}O_3$ could be estimated using the same empirical equations with the tolerance factor calculated from the averaged radii (B-site Mg^{2+} and Cr^{3+} in this case).[16] Bakken et al. suggested that nonstoichiometric materials like $A^{3+}BO_{3-\delta}$ could be viewed as an ideal solid solution of $A^{3+}B^{3+}O_3$

and $A^{3+}B^{2+}O_{2.5}$ with random mixing of B^{2+} and B^{3+} at the B-sites and oxygen and oxygen vacancy at the O-sites. Bakken calculated the free energy change from $A^{3+}B^{3+}O_3$ and $A^{3+}B^{2+}O_{2.5}$ to $A^{3+}BO_{3-\delta}$ as the entropy of mixing and left out any enthalpy effect.[35]

Both these treatments do not seem applicable to the current study. Prediction based on the first method is that $La_{0.7}Sr_{0.3}VO_3$ would react with H_2S while $La_{0.35}Sr_{0.65}TiO_3$ would hydrolyze to $La_2Ti_2O_7$ and $SrTiO_3$, which is contradictory to experiments. One outcome of the second treatment is that there will be local regions within the perovskite material that have excess of positive or negative charges, which do not correspond to the lowest energy state. In the authors' opinion, a more reasonable model for the doped perovskite might be that the distribution of alien ions (in this case La^{3+} and Sr^{2+} ions at the A-sites) follow random distribution while the multivalence ion (in this case Ti^{3+}/Ti^{4+} or V^{3+}/V^{4+} at the B-sites) will alter its valence and distribute according to the distribution of the A-site ions to maintain local charge neutrality. The validity of this treatment will be investigated by both theoretical calculation and experiments in future work.

Another important point is that the thermodynamic analysis made here is limited in that it only predicts the chemical stability of bulk materials. It does not provide any direct information about the stability of surface species (e.g., adsorbed sulfur) nor catalytic activity of the materials. This is clearly seen for the Ni–YSZ cermet anode: the equilibrium pH_2S/pH_2 ratio for bulk nickel sulfide at 950°C in H_2 fuel is as high as 10^{-2} ppm, while it is known that the Ni-based anode is poisoned by H_2S in the parts per million range.[36,37] It is generally believed that surface sulfide would be much more stable than bulk sulfide in low concentration of H_2S.[38] Whether the above thermodynamic analysis on bulk materials could be extended to include the surface effect (surface thermodynamics) is still under investigation.

Conclusions

The stability of various materials (metal carbides, borides, nitrides, silicides, sulfides, and complex oxides, etc.) in SOFC anode atmosphere containing H_2S was analyzed using principles of thermodynamics. The results help to rule out a large number of candidates such as most transition metal carbides, borides, nitrides, and silicides. Estimation of the thermochemical data for perovskite-structured oxide based on empirical equations provides valuable predictions about the stability of those materials. Further study is required to explain the stability of doped perovskite material and reveal the relationship between stability of surface species and the response of anode material to sulfur contaminants.

Acknowledgment

This work was supported by the Department of Energy NETL SECA Core Technology Program under award no. DE-FC26-04NT42219.

Georgia Institute of Technology assisted in meeting the publication costs of this article.

References

1. N. U. Pujare, K. W. Semkow, and A. F. Sammells, *J. Electrochem. Soc.*, **134**, 2639 (1987).
2. N. U. Pujare, K. J. Tsai, and A. F. Sammells, *J. Electrochem. Soc.*, **136**, 3662 (1989).
3. C. Yates and J. Winnick, *J. Electrochem. Soc.*, **146**, 2841 (1999).
4. S. Wang, M. Liu, and J. Winnick, *J. Solid State Electrochem.*, **5**, 188 (2001).
5. M. Liu, G. Wei, J. Luo, A. R. Sanger, and K. T. Chuang, *J. Electrochem. Soc.*, **150**, A1025 (2003).
6. G. Wei, J. Luo, A. R. Sanger, and K. T. Chuang, *J. Electrochem. Soc.*, **151**, A232 (2004).
7. L. Aguilar, S. Zha, S. Li, J. Winnick, and M. Liu, *Electrochem. Solid-State Lett.*, **7**, A324 (2004).
8. L. Aguilar, S. Zha, Z. Cheng, J. Winnick, and M. Liu, *J. Power Sources*, **135**, 17 (2004).
9. S. Zha, P. Tsang, Z. Cheng, and M. Liu, *J. Solid State Chem.*, **178**, 1844 (2005).
10. S. Zha, Z. Cheng, and M. Liu, *Electrochem. Solid-State Lett.*, **8**, A406 (2005).
11. H. Kim, J. M. Vohs, and R. J. Gorte, *Chem. Commun. (Cambridge)* **2001**, 2334.
12. H. He, R. J. Gorte, and J. M. Vohs, *Electrochem. Solid-State Lett.*, **8**, A279 (2005).
13. R. Mukundan, E. L. Brosha, and F. H. Garzon, *Electrochem. Solid-State Lett.*, **7**, A5 (2004).
14. O. Marina and J. Stevenson, in *2004 Office of Fossil Energy Fuel Cell Program Annual Report*, p. 90, Office of Fossil Energy, U.S. Department of Energy (2004).
15. H. Yokokawa, N. Sakai, T. Kawada, and M. Dokiya, *J. Electrochem. Soc.*, **138**, 1018 (1991).
16. H. Yokokawa, N. Sakai, T. Kawada, and M. Dokiya, *J. Electrochem. Soc.*, **138**, 2719 (1991).
17. Y. M. Choi, C. Compson, M. C. Lin, and M. Liu, *J. Alloys Compd.* In press.
18. M. W. Chase, Jr., C. A. Davies, J. R. Downey, Jr., D. J. Frurip, R. A. McDonald, and A. N. Syverud, *JANAF Thermochemical Tables*, 3rd ed., American Institute of Physics, New York (1986).
19. I. Barin, *Thermochemical Data of Pure Substances*, 3rd ed., VCH, Weinheim, Germany (1995).
20. A. Navrotsky, in *Structure and Bonding in Crystals*, Vol. II, M. O'Keeffe and A. Navrotsky, Editors, p. 71, Academic Press, New York (1981).
21. H. Yokokawa, T. Kawada, and M. Dokiya, *J. Am. Ceram. Soc.*, **72**, 152 (1989).
22. H. Yokokawa, N. Sakai, T. Kawada, and M. Dokiya, *J. Am. Ceram. Soc.*, **73**, 649 (1990).
23. J. Cheng and A. Navrotsky, *J. Mater. Res.*, **18**, 2501 (2003).
24. K. B. Helean, S. V. Ushakov, C. E. Brown, A. Navrotsky, J. Lian, R. C. Ewing, J. M. Farmer, and L. A. Boatner, *J. Solid State Chem.*, **177**, 1858 (2004).
25. J. Cheng and A. Navrotsky, *J. Solid State Chem.*, **177**, 126 (2004).
26. J. Cheng, A. Navrotsky, X.-D. Zhou, and H. U. Anderson, *J. Mater. Res.*, **20**, 191 (2005).
27. R. D. Shannon, *Acta Crystallogr., Sect. A: Cryst. Phys., Diffr., Theor. Gen. Crystallogr.*, **A32**, 751 (1976).
28. Z. Cheng, M. D. Sacks, and C.-A. Wang, *Ceram. Eng. Sci. Proc.*, **24**, 23 (2003).
29. A. W. Weimer, *Carbide, Nitride and Boride Materials Synthesis and Processing*, Chapman & Hall, London (1997).
30. O. A. Marina, N. L. Canfield, and J. W. Stevenson, *Solid State Ionics*, **149**, 21 (2002).
31. Z. Cheng, S. Zha, L. Aguilar, and M. Liu, *Solid State Ionics*, **176**, 1921 (2005).
32. S. Tao and J. T. S. Irvine, *J. Electrochem. Soc.*, **151**, A252 (2004).
33. O. Porat, C. Heremans, and H. L. Tuller, *Solid State Ionics*, **94**, 75 (1997).
34. D. C. LaMont, A. J. Gilligan, A. R. S. Darujati, A. S. Chellappa, and W. J. Thomson, *Appl. Catal., A*, **255**, 239 (2003).
35. E. Bakken, T. Norby, and S. Stolen, *J. Mater. Chem.*, **12**, 317 (2002).
36. N. Q. Minh and T. Takahashi, *Science and Technology of Ceramic Fuel Cells*, p. 147, Elsevier Science, Netherlands, (1995).
37. Y. Matsuzaki and I. Yasuda, *Solid State Ionics*, **132**, 261 (2000).
38. C. H. Bartholomew, P. K. Agrawal, and J. R. Katzer, *Adv. Catal.*, **31**, 135 (1982).